AIAA 2003–0789

The Effect of Spanwise-Modulated Disturbances on Transition in a 2-d Separated Boundary Layer

Olaf Marxen,
Ulrich Rist,
and Siegfried Wagner
Institut für Aerodynamik und Gasdynamik,
Universität Stuttgart, D-70550 Stuttgart, Germany

41st AIAA Aerospace Sciences Meeting and Exhibit
January 6–9, 2003/Reno, NV

The Effect of Spanwise-Modulated Disturbances on Transition in a 2-d Separated Boundary Layer

Olaf Marxen*,
Ulrich Rist†,
and Siegfried Wagner‡
Institut für Aerodynamik und Gasdynamik,
Universität Stuttgart, D-70550 Stuttgart, Germany

A laminar boundary layer separates in a region of adverse pressure gradient on a flat plate and undergoes transition. The detached shear-layer rolls up into spanwise vortices that rapidly breakdown into small-scale turbulence. Finally the turbulent boundary layer reattaches, forming a laminar separation bubble. The development and role of three-dimensional disturbances for the transition in such a separation bubble is studied by means of direct numerical simulation with controlled disturbance input. It is shown that the level of incoming 3-d perturbations is not relevant in the present case due to an absolute instability of these disturbances in the region of shear-layer roll-up. In particular this is true for steady disturbances up to very high amplitudes. Furthermore, the development of such steady streaks is attributed to strong transient growth after their generation by non-linear interaction of traveling waves in the region of favorable pressure gradient. Numerical results are confirmed by a comparison with experimental data.

Introduction

TRANSITION to turbulence in a two-dimensional separated boundary layer often leads to reattachment of the turbulent boundary-layer and the formation of a laminar separation bubble (LSB). In environments with a low level of fluctating disturbances, the transition process is governed by strong amplification of these disturbances. Such a scenario is typical for a pressure-induced LSB, e.g. found on a (glider) wing in free flight or for an experiment where the region of pressure rise is preceded by a favourable pressure gradient that damps out unsteady perturbations.[1] In the region of adverse pressure gradient, disturbances are subject to strong amplification, and their saturation leads to shear-layer roll-up and vortex shedding. This vortex shedding is often essentially a two-dimensional phenomenon (i.e. strong spanwise coherence of the vortex structure), caused by either spanwise constant (2-d) small-amplitude waves or by spanwise-harmonic (3-d) waves with small obliqueness angles in an otherwise undisturbed flow. According to a classification by Rist & Maucher,[2] amplification of these waves can proceed via a gradual switch-over from a viscous wall-mode instability (so called Tollmien-Schlichting (TS) instability) towards an inviscid free shear-layer type instability (Kelvin-Helmholtz instability), distinguishable by the position and strength of the maximum in the disturbance-amplitude function.

Considerable discussion is still going on as to the origin and role of disturbances with spanwise variation in a LSB. Two distinct forms of 3-d disturbances are commonly observed: steady and highly-fluctuating. In the past, presence of steady perturbations in separated flows was commonly attributed to Görtler vortices.[3–5] Amplification of such streamwise vortices is caused by the effect of streamline curvature.

Research of bypass transition in zero pressure gradient boundary-layers revealed the possibility of transient growth of steady spanwise disturbances that are often referred to as streaks.[6] Presence of streaks in conjunction with separated flows was experimentally observed by Watmuff.[1] The development of such streaks in separated boundary-layers and their relation to transient growth has only recently been studied experimentally and theoretically.[7]

Growth of fluctuating perturbations is occasionally attributed to a (classical) secondary instability known from K-type boundary-layer transition with its peak-valley splitting.[8] However, it was concluded by Rist[9] that such a scenario, analysable by Floquet theory, is unlikely to be observed in LSB's. Instead, breakdown of weakly-oblique traveling waves as the probably fastest route to turbulence in certain types of separation bubbles is proposed. A mechanism of absolute secondary instability of three-dimensional disturbances in separation bubbles was discovered by Maucher *et al.*[10] for fairly strong pressure gradi-

*Research Assistant.
†Senior Research Scientist.
‡Professor, Member AIAA.

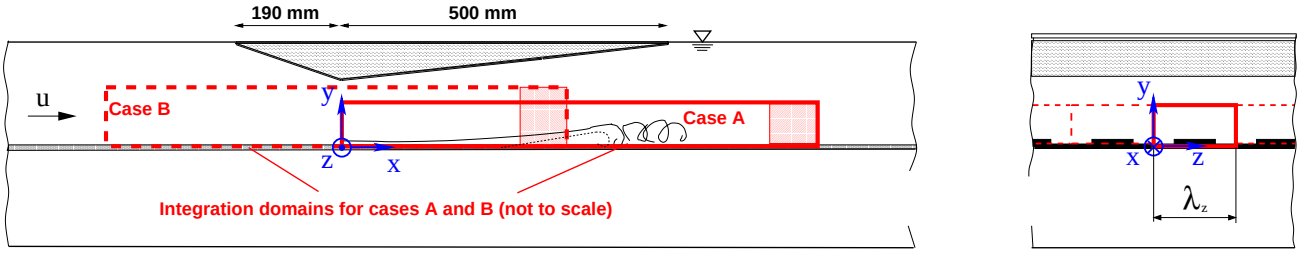

a) Experimental set-up and numerical integration domains.

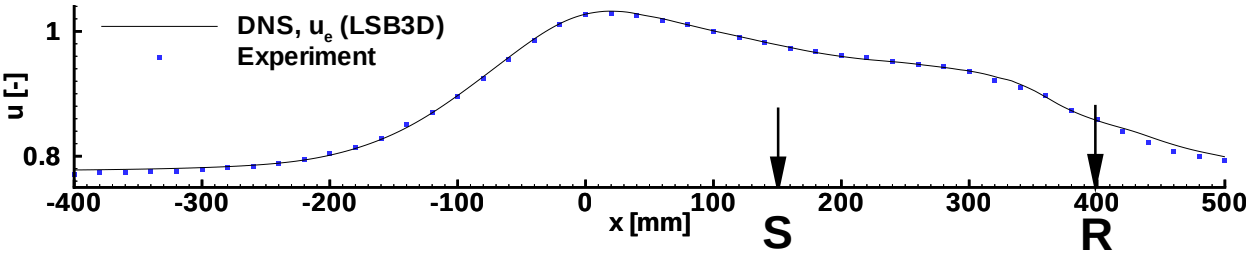

b) streamwise velocity at a constant distance from the wall ($y = 50\ mm$).

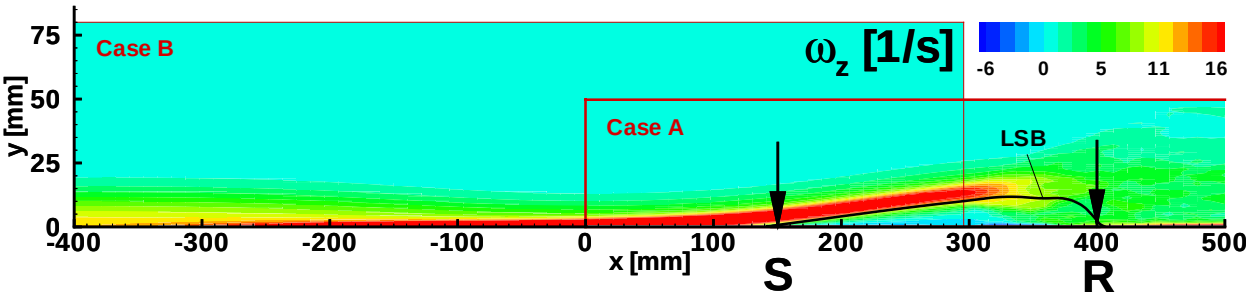

c) contours of the spanwise vorticiy $\omega_z = \partial u/\partial y - \partial v/\partial x$ from DNS ($LSB3D$) together with the dividing streamline.

Fig. 1 Experimental & numerical set-up (a) and time- & spanwise-averaged flow quantities (b, c).

ents and/or high local Reynolds number based on the displacement thickness δ_1 at separation $Re_{\delta_1}^{x=x_s}$. In Ref. 11 a somewhat similar mechanism of absolute instability is proposed, leading to sudden transition with immediate occurence of three-dimensionality. However, it was stated there that such a mechanism is not analysable in terms of primary or secondary instability.

The present study shall provide an insight into possible instability mechanisms leading to amplification of spanwise-harmonic disturbances in a LSB and their importance for the transition process. It is divided into two parts, the first being concerned with fluctuating disturbances, whereas the second part deals with steady distortions. The subject is studied by means of direct numerical simulations (DNS) with controlled disturbance input, designed to closely model an experiment carried out at the Institut für Aerodynamik und Gasdynamik (IAG), which serves as a reference case.

Description of the Flow

The reference case is defined by an experimental set-up specified in detail in Ref. 12, 13. Only a brief description shall be given here. A flat plate was mounted in the free stream ($U_\infty = 0.125 m/s$) of the test section of a laminar water channel. A streamwise pressure gradient was imposed on the flat-plate boundary layer by a displacement body, inducing a region of favorable pressure gradient followed by a pressure rise (Fig. 1 (a), (b)). In the region of adverse pressure gradient (starting at $x \approx 0\ mm$), a laminar separation bubble develops (Fig. 1(c)) between the points of separation (S) and mean reattachment (R).

The transition experiment is performed with controlled disturbance input. A 2-d time-harmonic perturbation is introduced upstream of the displacement body ($x = -230\ mm$) by an oscillating wire (fundamental frequency $f_0 = 1.1\ Hz$). Additionally, 3-d disturbances are imposed by placing thin ($1.0\ mm$) metal plates (spacers) regularly underneath the wire (fundamental spanwise wavelength $\lambda_z = 58\ mm$). Special experimental procedures for data acquisition[12] allowed for spectral decomposition in time and spanwise direction.

For calculations, general physical parameters of the flow are chosen to match this set-up as close as pos-

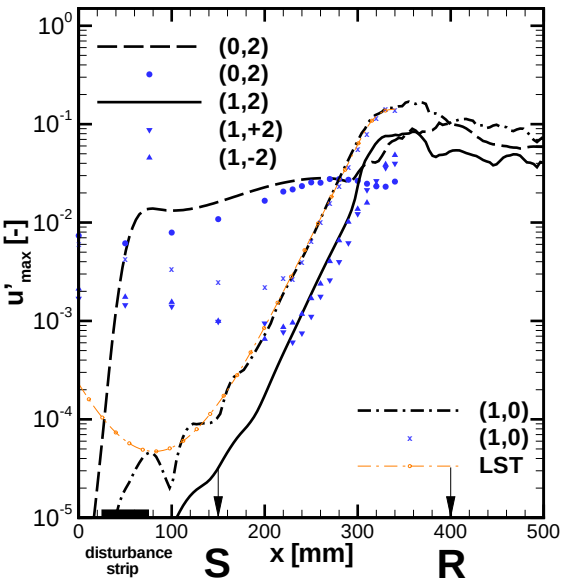

Fig. 2 Amplification of the max. 2-d and 3-d streamwise velocity fluctuation u'_{max}. DNS (lines), LDA (symbols), and LST (taken from Ref. 13).

sible. At a streamwise position $x = -400\ mm$ the observed boundary-layer profile can be approximated by a Falkner-Skan similarity solution ($Re_{\delta_1} = 900$, $\beta = 1.03$) and is used as inflow condition. In contrast to the experiment, in numerical simulations different combinations of the disturbance input are chosen. Velocities are made dimensionless using a pseudo potential-velocity at the wall in the narrowest cross section ($x = 0\ mm$). The procedure to obtain this velocity is described in detail in Marxen *et al.*[13]

In previous works,[12,13] it was shown that numerical results and measurements obtained by Laser-Doppler Anometry (LDA) as well as predictions from linear stability theory (LST) agree very well for time-averaged (Fig. 1(b)) and 2-d time-harmonic quantities (Fig. 2). In this study, further insight into the impact of spanwise-modulated disturbances of small to medium amplitude on the transition process shall be gathered. Results from Ref. 13 serve as a reference and physical processes occuring in this reference case are shortly described in the following.

The first section of the LSB is dominated by a primary convective instability of a two-dimensional Tollmien-Schlichting (TS) wave of fundamental frequency. Fig. 2 (taken from Marxen *et al.*[13]) shows that the TS wave $(1, 0)$ is strongly amplified in the region of adverse pressure gradient. Good agreement of both experimental and numerical results with linear stability theory (LST) from $x = 230\ mm$ onwards confirms the primary convective nature of this disturbance. Breakdown to small-scale 3-d turbulence occurs around the position of saturation of the fundamental wave. In Ref. 13 it was stated that oblique waves eventually cause breakdown to turbulence. These waves emerge from non-linear interaction of a large steady 3-d and the fundamental 2-d disturbance as it was found by additional calculations.

The present study serves to prove the above stated picture of the transition process in the LSB by discussing the results of these additional calculations and their implications. In addition, conclusions drawn from these calculations then lead to the possibility to clarify the origin of steady disturbances and their impact on the transition process in LSB's. Since time-harmonic disturbances non-linearly generate steady ones, in most cases it is not meanigful to exclude one or the other of these disturbances in the calculations by e.g. solving time-averaged equations.

Numerical Method

Spatial direct numerical simulation of the three-dimensional incompressible Navier-Stokes equations serves to compute the accelerated and decelerated boundary-layer described in the previous section. Two different methods are applied for the examination of fluctuating (case A) and steady (case B) three-dimensional disturbances. Both methods use finite differences on a cartesian grid for downstream and wall-normal discretization, while a spectral ansatz is applied in spanwise direction. A fourth-order Runge-Kutta scheme is used for time integration. Upstream of the outflow boundary a buffer domain smoothly returns the flow to a steady laminar state. An additional damping zone at the upper boundary prevents reflections of disturbances in the turbulent part of the boundary layer. Disturbances of any frequency are introduced via blowing and suction at the wall through a disturbance strip. To reduce computational effort, spanwise symmetry is assumed for calculations.

Case A makes use of fourth-order accurate finite differences on an equidistant grid. Since this method is applied when the integration domain contains the whole separation bubble, inviscid-viscous interaction due to boundary-layer displacement must be accounted for. The displacement depends on the size of the LSB that is not known a priori, but instead is a result of the calculation. Numerical method A is described in detail in Ref. 13, 14.

The method for case B is of sixth-order accuracy and allows for grid stretching in the wall-normal direction. For integration domains that contain only the first part of the LSB, it is meaningful to distinguish between a 2-d stationary base flow and unsteady perturbations, so that a disturbance formulation is applicable. This will be further explained in a later section. Numerical method B is described in detail in Ref. 15. Compared to there, the calculation of coefficients for finite differences is altered to allow for non-equidistant grids in wall-normal direction.

A double Fourier transform in time and spanwise direction of data sets from measurements or simulation yields disturbance amplitudes and phases. Below, the notation (h, k) will be used to specify the modes, with h and k denoting wave-number coefficients in time and spanwise direction, respectively.

For simulations of case A, the separation bubble showed low-frequency oscillations (so-called flapping) so that the Fourier analysis had to be carried out using a Hanning-window function to suppress aliasing effects. Four periods of the fundamental frequency where used in the analysis. The subharmonic was checked to have low amplitude and taken as prove that frequencies of the flapping and of the shedding were indeed well separated.

Time-Harmonic 3-d Disturbances

Since turbulence is characterized by highly fluctuating three-dimensional disturbances, in this section the role of unsteady spanwise-harmonic disturbances for the transition process shall be clarified. This is achieved by a variation of number, type and amplitude of three-dimensional disturbance input.

Despite the importance of 3-d perturbations for the breakdown process, transition is dominated by the two-dimensional TS wave.[13] However, the role of this type of disturbance is clear, as it was already shown by Augustin *et al.*[16] that the initial amplitude of the fundamental 2-d wave is responsible for the overall size of a forced LSB. Therefore, no attempt to vary its amplitude was made here.

Test Cases *A*

In all cases A a small-amplitude two-dimensional time-harmonic wave $(1, 0)$ with the same amplitude is forced upstream of the LSB. Additional steady and/or time-harmonic as well as spanwise-harmonic disturbances are excited with different amplitudes. Disturbance amplitudes for the wall-normal velocity for several calculations are given in table 1. The notation used gives a hint whether disturbance amplitude is high (superscript) or low (subscript).

The integration domain (Fig. 1(a)) starts at $x = 0\ mm$. Its streamwise and wall-normal extent was $x_L = 812\ mm$ and $y_L = 50\ mm$, respectively. The spanwise extent is a single spacer wavelength. The number of grid points n and modes k is $n_x \times n_y \times k_z =$ $1778 \times 185 \times 27$. The discretization in x results in approximately 120 grid points per streamwise wavelength of the fundamental wave. Last 246 grid points in x and the topmost 20 grid points in y are used as buffer zones, where the flow is gradually ramped to a laminar state. Resolution in time was 600 time steps per fundamental period. The disturbance strip was 120 grid points in length and centered at $n_x = 120$.

Table 1 Disturbance v-amplitudes for cases *A*.

Case	(1,0)	(0,2)	(1,2)
LSB3D	7×10^{-6}	1.82×10^{-3}	–
$A^{\star}_{02}$	9×10^{-6}	4×10^{-4}	–
A^{02}	9×10^{-6}	6.8×10^{-4}	–
A^{02}_{12}	9×10^{-6}	6.8×10^{-4}	2×10^{-5}
A_{02-12}	9×10^{-6}	1.8×10^{-4}	2×10^{-5}
$A_{no\ 3D}$	9×10^{-6}	–	–

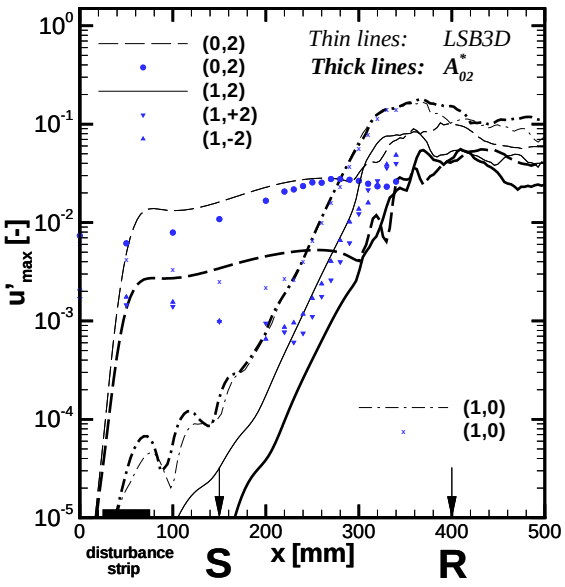

Fig. 3 Same as Fig. 2. Comparison of reference case $LSB3D$ with case $A^{\star}_{02}$.

Before discussing the results, the concept of non-linear generation is briefly explained. Resulting from the non-linear terms in the Navier-Stokes equations, two disturbances of the streamwise velocity $u_1 = \hat{U}_1 \cdot e^{h_1 \cdot t + k_1 \cdot z}$ and $u_2 = \hat{U}_2 \cdot e^{h_2 \cdot t + k_2 \cdot z}$ cause a disturbance $u_1 \cdot u_2 = \hat{U}_1 \hat{U}_2 \cdot e^{(h_1 \pm h_2) \cdot t + (k_1 \mp k_2) \cdot z}$, e.g. mode $(1, 0)$ and mode $(0, 2)$ will result in a mode $(1, 2)$ with an amplitude given roughly by the product of amplitudes of the generating modes. This example indicates that steady 3-d disturbances can play a role in generation of certain types of 3-d unsteady perturbations.

Results

A comparison of reference case $LSB3D$ with a simulation with lower amplitude of the steady disturbance $(0, 2)$ case $A^{\star}_{02}$ is shown in Fig. 3. Although mode $(0, 2)$ reaches high u-amplitudes (>3% with respect to the local free-stream velocity) in the reference case, the transition mechanism remains the same. In both cases mode $(1, 0)$ possesses the same amplitude, amplification rate and saturation level. The 3-d modes $(0, 2)$ & $(1, 2)$ in case $A^{\star}_{02}$ show an equal amplification and a comparable saturation level as in the reference case, however displaced to a lower amplitude in the laminar part of the LSB ($x < 300\ mm$).

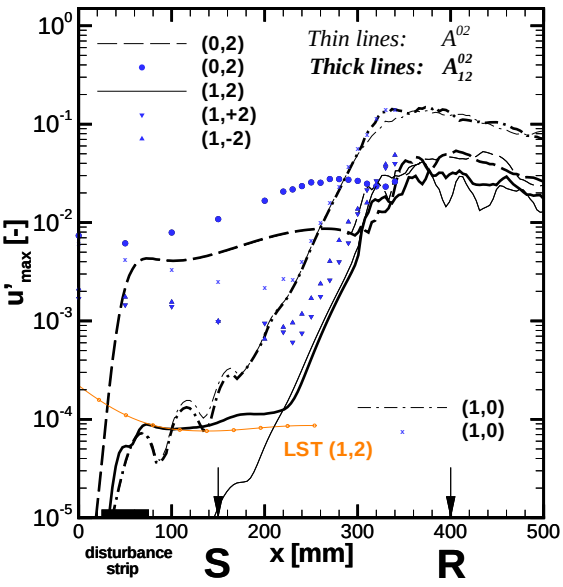

Fig. 4 Same as Fig. 2. Comparison of cases A^{02} and A^{02}_{12}.

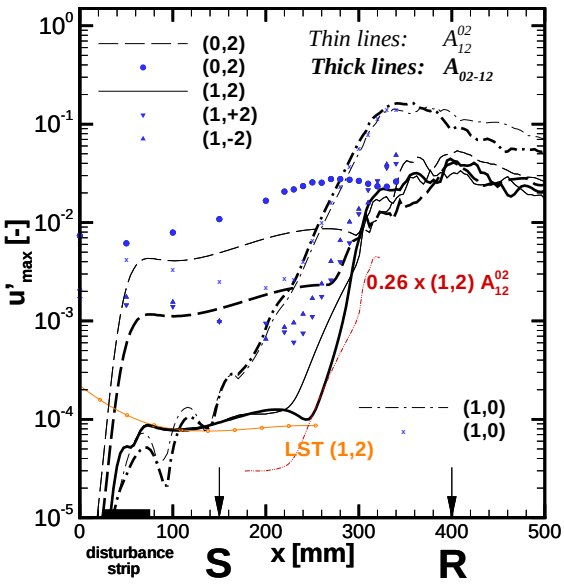

Fig. 5 Same as Fig. 2. Comparison of cases A^{02}_{12} and A_{02-12}.

As a consequence, amplification of mode $(1,2)$ cannot be attributed to secondary instability caused by three-dimensional distortion of the mean flow through the large steady disturbance, because the growth rate would necessarily depend on the strength of the distortion of the mean flow and thus on the amplitude of the steady disturbance. Instead, no change in amplifcation rate is observed, since amplitude curves of disturbances $(1,2)$ are parallel in Fig. 3.

To exclude a dependency on the initial amplitude of mode $(1,2)$, which is different in both previous cases, an additional disturbance $(1,2)$ is introduced (case A^{02}_{12} versus case A^{02}, both with a slightly different amplitude of the steady disturbance). It can be seen in Fig. 4 that from the streamwise position $x = 220\ mm$ onwards, equal development of mode $(1,2)$ is observable, excluding a dependency from initial amplitude of mode $(1,2)$.

Furthermore, onset of strong growth of mode $(1,2)$ cannot be explained by linear theory, which predicts damping downstream of $x = 220\ mm$ (Fig. 4, see also Fig. 5 in Ref. 13). The region of primary instability for this perturbation is confined to a region close to the separation point, which can be ascribed to the high obliqueness angle of this wave ($\approx 60°$).

The reason for deviation of amplification of mode $(1,2)$ from predictions of LST upstream of $x = 220\ mm$ (Fig. 4) is not known. Non-parallelity of the base flow might play a strong role for highly oblique waves which is neglected in the LST approach used here.[13] Despite the deviation towards higher amplification rates, growth still remains fairly small when compared to the growth due to non-linear interaction.

If the amplitude of the steady disturbance mode $(0,2)$ is considerably reduced (case A_{02-12}), strong growth of mode $(1,2)$ is delayed further downstream (Fig. 5). However, since amplification is slightly stronger now, saturation level and position for mode $(1,2)$ show no significant difference to the previous case A^{02}_{12}. Parallel amplitude development is confined to a small streamwise region as illustrated by a multiplication of amplitude curve $(1,2)$ for case A^{02}_{12} by a factor $1.8/6.8 \approx 0.26$.

Strong amplification of mode $(1,2)$ in case A_{02-12} is observable from a streamwise position onwards where the TS wave has already gained high amplitude (> 1 %), and thus in later stages of the transition process. This strong amplification is confined to an even smaller streamwise region as before and therefore transition would appear sudden when amplitudes are not plotted in a logarithmic scale. This strongly resembles the secondary instability mechanism proposed by Maucher *et al.*[10]

When switching off all three-dimensional disturbances (case $A_{no\ 3D}$), it turns out that indeed such a mechanism of absolute instability with respect to 3-d perturbations is at work, since 3-d disturbances are not convected downstream and the development of modes $(1,0)$ & $(1,2)$ remains essentially the same (Fig. 6). This gives the last prove that transition in the reference case is in fact a result of an absolute secondary instability of three-dimensional disturbances in the presence of a large-amplitude TS wave as stated in section .

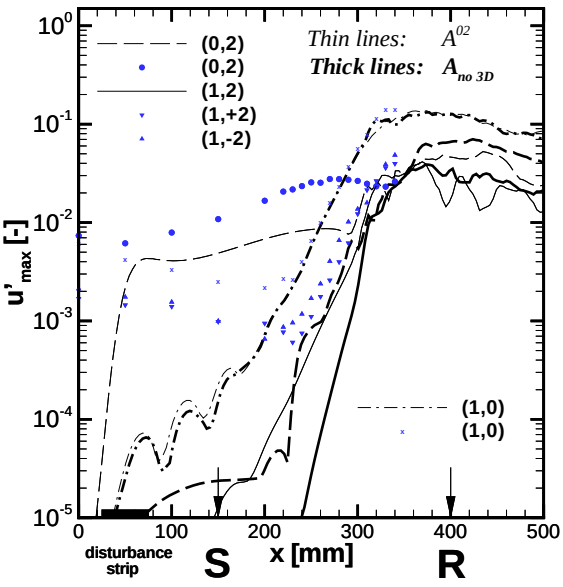

Fig. 6 Same as Fig. 2. Comparison of cases A^{02} and $A_{no\ 3D}$.

Discussion

A strong spanwise modulation of the flow field in the first part of the LSB does not exert an important influence on 2-d primary instability characteristics, as can be seen from good agreement of the development of the fundamental TS wave $(1,0)$ with LST in all cases. This is not suprising, since the only influence imaginable would be through a mean flow deformation caused by mode $(0,2)$, which should be of the order $\leq \left(3 \cdot 10^{-2}\right)^2 \approx 10^{-3}$ which is at least two orders of magnitude below the base flow velocity at the y-position of the maximum of mode $(1,0)$. This observation is in line with results from Mendonça *et al.*[17] that showed a suppression of amplification of TS waves only for steady spanwise perturbations with amplitudes above 10%.

Secondary instability with respect to the steady spanwise perturbation is not observable in any case with disturbance amplitudes for the streamwise velocity up to 3 %. This is consistent with observations of secondary instability of Görtler vortices[18] with a necessary amplitude > 10 % or for boundary-layer streaks, where an even higher amplitude (>20 %) seems necessary.[19]

The present case with a Reynolds number based on the momentum thickness δ_2 at separation $Re_{\delta_2}^{x=x_s} = 305$ and a deceleration parameter $P = {\delta_2}^2/\nu \cdot \Delta u/\Delta x \approx -0.23$ is comparable to Gaster's[20] case IV, series I. It therefore can be put in between the studies by Wilson and Pauley[5] with $Re_{\delta_2} = 430$, $P = -0.28$ and Spalart and Strelets[11] with $Re_{\delta_2} = 180$, $P = -0.1$.

A transition scenario is introduced here where a moderately growing large steady spanwise-harmonic perturbation together with a strongly amplified two-dimensional TS wave causes breakdown to turbulence by mere non-linear interaction. However, switching off the 3-d disturbance input revelead that in fact a transition mechanism described by Maucher *et al.*[10] is in operation. Furthermore, there is indication that it might be the same mechanism as in Ref. 11, since there as well as in the present case, shear-layer type instability (Kelvin-Helmholtz) is involved together with rapid onset of three-dimensionality. The only difference concerns the origin of 2-d disturbance waves which are explicitely forced in the present case while forcing is absent in the study of Spalart and Strelets.[11] It is argued there that a receptivity mechanism might be present, acting to transform pressure fluctuations into streamwise waves. This hypothesis is further supported by the fact that the disturbance level does not fall below values that are on the same order as the disturbance input here (see Fig. 6 in Ref. 11). Time-growing disturbances in conjunction with vortex shedding (which is also present here as a result of saturation of TS waves) were also observed by Pauley,[4] but attributed to start-up transients and not related to an absolute instability.

One should not forget that despite the presence of a large steady mode $(0,2)$, it is the traveling oblique wave $(1,2)$ that serves to break-up the spanwise vortex rapidly into small-scale structures. The presence of a large steady disturbance does only help to explain the growth rate of mode $(1,2)$ observed experimentally and to show that experimental conditions can accurately be reproduced by DNS, but it does not play an essential role in the transition process in this LSB.

Development of Steady 3-d Disturbances

For calculations considered in this section, results from previously described calculations (however, with different discretization as will be seen in the next section) were time-averaged and used as a stationary base flow for subsequent numerical simulations. Conclusions drawn in the last section justify such a procedure up to a streamwise position close to the transition location ($x = 320\ mm$).

In the last section, it was found that even large steady 3-d disturbances do not change the stability behavior of the flow field. This stability behavior is known to be very sensitive with respect to the shape of e.g. the u-velocity profile. Thus, mean properties were not affected and allowed to run a case without 3-d disturbance input ($A_{no\ 3D}$).

As can be seen from Fig. 6, up to a streamwise position of $x = 200\ mm$, disturbances remain below 10^{-3}, so their possible contribution to the base flow due to non-linear interaction schould be on the or-

der of 10^{-6}. A solution to the full three-dimensional Navier-Stokes equations that is converged to a steady two-dimensional state with an error of $O(10^{-6})$ can be well regarded as a stationary two-dimensional solution of the Navier-Stokes equations and is therefore usable as a base flow in subsequent disturbance calculations.

It should be noted that the time-averaged flow field in the first part of the LSB can only be computed once the exact pressure distribution is known. However, this distribution is a result of inviscid-viscous interaction of the separation bubble with the mean flow (i.e. the pressure plateau is a result of this effect), which implies the necessity of including the whole separation bubble inside the domain to obtain the true pressure distribution.

With detailed measurements available, it might be possible that the measured velocity distribution (Fig. 1(b)) at the upper boundary of the integration domain would be usable for a base flow calculation leading to a steady state with reverse flow at the outflow boundary, instead of the time-averaging procedure used here. However, it is believed that this reverse flow would pose a serious problem for specification of outflow boundary conditions. In the present ansatz, this problem is avoided since boundary conditions are only necessary for disturbance quantities, which can simply be ramped down to zero using the buffer domain technique.

Test Cases *B*

Several combinations of disturbance excitation constitute the test cases of this section. Disturbance amplitudes for the wall-normal velocity are given in table 2. Since in the experiment mode $(0,2)$ is the largest disturbance observable in the first part of the LSB (Fig. 7), all cases B where especially designed to study the behavior of that mode.

The inflow boundary is placed at a position upstream of the displacement body ($x_L = -400\ mm$), before strong acceleration sets in (Fig. 1(b)). The outflow boundary was located at $x = 295\ mm$. The wall-normal extent of the integration domain was raised to $y_L = 80\ mm$. Its spanwise extent again is a single spacer wavelength. The number of grid-points n and modes k was $n_x \times n_y \times k_z = 1538 \times 241 \times 5$, with 128 grid points in x and 10 grid points in y used for a buffer

Table 2 Disturbance v-amplitudes for cases *B*.

Case	(0,1)	(0,2)	(1,0)	(1,1)	(1,2)
B^{01}	0.0118	–	–	–	–
B_{01}	0.0040	–	–	–	–
B^{02}	–	0.026	–	–	–
B_{02}	–	0.0029	–	–	–
B^{11}	–	–	–	0.02	–
B_{11}	–	–	–	0.0067	–
B_{10-12}	–	–	0.010	–	0.010

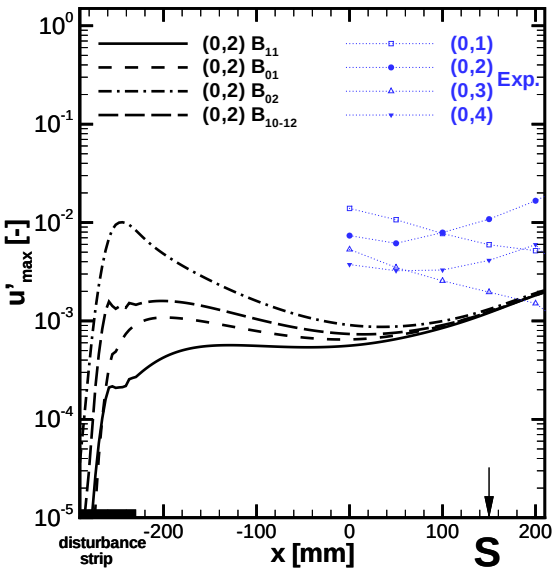

Fig. 7 Amplification of the max. steady spanwise-harmonic velocity $u'_{max}(0,k)$. DNS (lines) and LDA (symbols). Comparison of all cases B_{xx}.

zone at the outflow and upper boundary, respectively.

Discretization in x results in approximately 128 grid points per streamwise wavelength of the fundamental wave. Low resolution in spanwise direction is justified since no breakdown to turbulence occurs in the calculations of this section. Therefore, beside the generation of disturbance modes by non-linear interaction, no further mutual influence of modes took place. In wall-normal direction grid points were clustered at the wall according to the following formula ($1 \le j \le n_y$):

$$y_j = y_L \left((1-\kappa) \cdot \left(\frac{j-1}{n_y - 1} \right)^3 + \kappa \cdot \left(\frac{j-1}{n_y - 1} \right) \right) \quad (1)$$

In the presented calculations, κ was chosen to be 0.1562, resulting in a ≈ 5.2 times shorter wall-distance of the wall-next grid point compared to an equidistant spacing. Resolution in time was raised to 900 time steps per fundamental period. Calculating up to the 20th period of the fundamental frequency proved to be sufficient to get converged results for the steady disturbances. This was checked by a calculation up to the 120th period which did not visibly differ from the presented results, and which showed a difference between results from one period to the next of $\approx 10^{-8}$ for the steady perturbations. To lower the difference by one order of magnitude took approximately 50 periods. The disturbance strip was 128 grid points in length and centered at $n_x = 320$.

Results

A comparison of disturbance amplitude development of all four cases reveals that the initial behavior

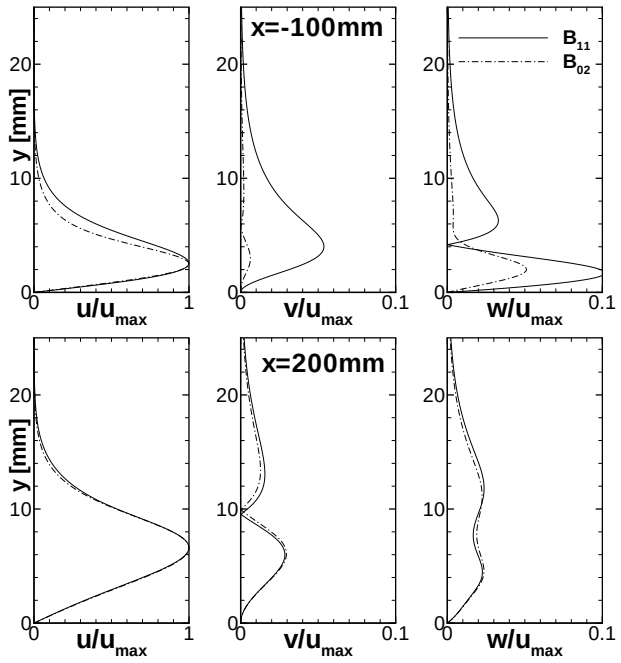

Fig. 8 Velocity amplitudes of mode $(0,2)$, normalized by their respective u'_{max}. Comparison of case B_{11} and B_{02}.

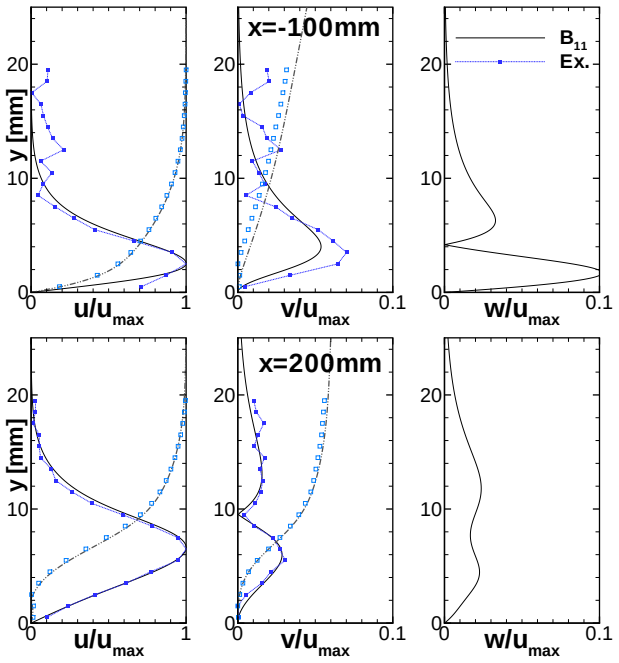

Fig. 9 Same as Fig. 8. Comparison of case B_{11} with measurements. In addition, mean flow quantities $(0,0)$ are also shown.

of the maximum streamwise velocity perturbation differs considerably from case to case (Fig. 7). Except for case B_{11} all calculations predict damping of the disturbance at first. After a long transient downstream development, differences in amplification rates become less pronounced until the same disturbance development is reached from $x \approx 150\ mm$ onwards. In addition, this final state shows the same amplification rate as in the experiment.

An explanation for the initially different behavior can be derived from looking at the wall-normal amplitude distributions. These are shown for two cases in Fig. 8 for all three velocity componentes at two streamwise positions ($x = -100\ mm$ and $x = 200\ mm$). At the first position, both cases show considerably different amplitude functions for the wall-normal velocity v and the spanwise velocity w. In case B_{11}, a streamwise vortex is developed, which can be seen from the fact that w changes its sign whereas v keeps the same sign for all y. In contrast, the perturbation in case B_{02} is merely a streak. Despite strong differences in v and w, it is remarkable how similar amplitude functions for u look in both cases.

In Fig. 9 the same amplitude distributions for case B_{11} are compared with experimental results. Fair agreement at the upstream position shows that it is very likely that steady perturbations observed in the experiment, are indeed a result of non-linear generation caused by a fluctuating disturbance, e.g. $(1,1)$. This hypothesis will further be justified below. At the second x-position, which is already inside the separation region, agreement is almost perfect, even for the very small v-amplitude.

A remarkable feature of the disturbances is that in contrast to TS-like perturbations, which show the same order of magnitude for both u and v (and exactly the same amplitude towards the edge of the boundary layer), v- and w-amplitude of the steady disturbance are considerable lower than the u-amplitude (more than one order of magnitude – note the different axis scaling in Fig. 8, 9). Since the same relation is seen for base flow quantities u and v , it appears appropriate to introduce a boundary-layer scaling for v and w. This is in line with analysis of Görtler flows.[18]

To confirm the hypothesis from above about the origin of mode $(0,2)$, simulations B^{01} & B^{02} with higher disturbance amplitudes are carried out. As can be seen in Fig. 10, perfect agreement with the experiment for mode $(0,2)$ is observed now in case B^{01}. However, this calculation predicts too high an amplitude for mode $(0,1)$.

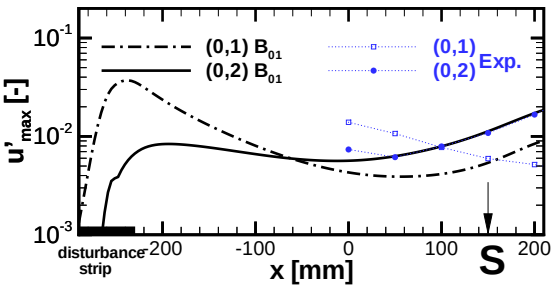

Fig. 10 Same as Fig. 7. Comparison of case B^{01} with measurements.

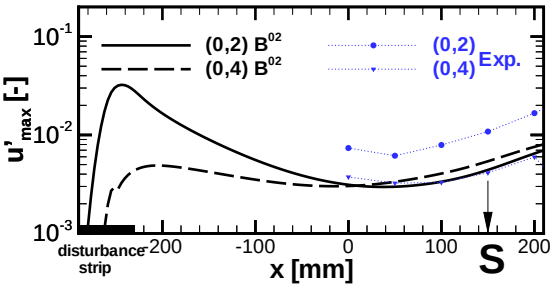

Fig. 11 Same as Fig. 7. Comparison of case B^{02} with measurements.

In contrast, it was not possible to raise the amplitude high enough so that the experimentally observed level could be reached, because non-linear effects appeared to set in, resulting in a different behavior of that perturbation. But even on the slightly to lower level shown in Fig. 11, a far too large mode $(0,4)$ is developed. Thus, both cases are unable to model the situation observed experimentally. Interaction of modes $(1,0)$ and $(1,2)$ (case B_{10-12}) would also be appropriate but gives slightly less favorable comparison to the experiment than case B_{11} at upstream x-positions. Besides, a higher amplitude of both generating modes would be necessary.

Finally, a simulation with adapted amplitude of mode $(1,1)$ was run (case B^{11}). Results are compared against measurements in Fig. 12. It can be seen that not only predicted growth rate and amplitude of mode $(0,2)$ favorably compare with experimental results, but also amplitude level and decay rate of the disturbed mode $(1,1)$ match quite well.

Discussion

Four distinct methods for disturbance input of a steady spanwise-harmonic showed different initial behavior, but developed downstream towards the same state. No difference was seen in final shape and growth rate of the disturbance, no matter whether it arose out of a vortex or out of a streak. The development of the steady disturbance inside the separation bubble can therefore be considered to be independent of initial condition, however only after a long transient region of disturbance development. This indicates that a prefered state (e.g. in the sense of the least damped state) is reached inside the LSB, supporting the idea of a Görtler instability to exist. However, as can be seen from the amplitude function inside the bubble, such a state is not necessarily a vortex as predicted for a Blasius boundary layer on a curved surface.[18]

From the favorable comparison of numerical results with measurements it can be concluded that the steady disturbance $(0,2)$ is indeed a spanwise-harmonic wave and not part of a localized structure, justifying the Fourier ansatz and the low spanwise resolution in the

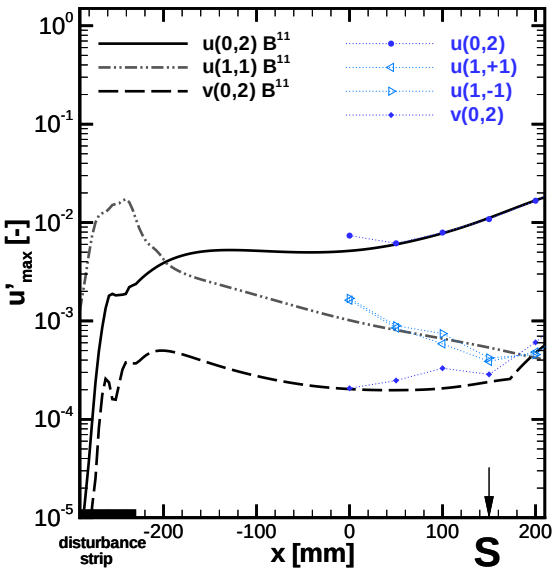

Fig. 12 Comparison of case B^{11} with measurements for streamwise & wall-normal velocities.

DNS. Furthermore, this indicates that despite its fairly large amplitude of up to ≈ 3 % of the free-stream velocity, growth of mode $(0,2)$ can still be considered to be linear. A comparison of cases B_{11} and B^{11} further supports this hypothesis by showing the same development independent of amplitude. This is in line with observations of Görtler vortices in Blasius flow, which non-linearly saturate only at an amplitude of 10 %.[18]

One possible explanation for the fact that steady disturbances need a much higher amplitude for saturation to occur when compared to traveling waves (e.g. TS waves) might be given by the large difference between maximum amplitudes of u on the one hand and v, w on the other hand. It was already stated above that for a TS-wave u, v are of the same order of magnitude (visible through joint exponential decay in y-direction at the edge of the boundary layer, see e.g. Fig. 6 in Ref. 13), whereas for the streaks a boundary-layer scaling (factor $\sqrt{Re}$) seems appropriate: the u-disturbance is of the same order as the base flow u, while the v-disturbance is of the same order as the base flow v if both are scaled by the respective u_{max}.

As emphasized before, amplitude functions for u look similar in all cases even at upstream x-positions, wereas v, w can be considarably different. This clearly demonstrates that fairly good agreement of u-amplitude functions with experimental data is not sufficient to determine the type of disturbance and thus to use it for validation purposes, as it is often done in studies of transient growth (see e.g. Fig. 1 in Ref. 19). Furthermore, it stresses the need for measurements of at least two but better all three velocity

components for studies of transient growth. Otherwise, such a comparison can be misleading, since as demonstrated before, the same u-amplitude function can either lead to growth or decay, depending on initial v and w shape and amplitude (when normalized by u_{max}). The streamwise distance of transient growth can be very long, here it was about 100 times the boundary-layer displacement thickness at $x = 0\,mm$.

It is often argued that the stabilizing influence of a region of favorable pressure gradient can serve to damp out disturbances.[1] This is definitely true for fluctuating disturbances as can be seen from the decay of mode $(1, 1)$ in Fig. 12. However, this is not always true for steady perturbations that might only slowly decay or even be amplified due to transient growth. This could be the reason for the occurence of streaks observed in similar conditions as the present ones[1] for which an explanation was not yet found.

Conclusions

In the present study, the role of three-dimensional steady disturbances and traveling waves with high-obliqueness angle could further be clarified by means of direct numerical simulation. Starting from a reference case, a variation of initial amplitude of steady and unsteady three-dimensional perturbations was performed to study the influence of different combinations of disturbance input.

It was shown that steady spanwise harmonic perturbations up to 3 % amplitude do not influence the transition process in the LSB under consideration. Since steady perturbations typically possess growth rates that are considerably lower[11,17] than those of traveling waves in LSB's, it is very unlikely that these disturbances gain a sufficiently high amplitude (i.e. > 10 %) to dominate directly the transition process by either suppressing TS wave growth[17] and therefore delaying transition or via a secondary instability[18,19] resulting in transition enhancement. Instead, unless very strong steady 3-d forcing is applied (e.g. Ref. 21), the traveling wave will always win over the steady disturbance.

Beside a direct influence, a large steady disturbance had hardly any effect on the development of the fundamental 2-d TS wave. In particular, no influence was seen on transition location, which is attributed to the effect of the 2-d wave. This is consistent with the type of secondary absolute instability suggested by Maucher *et al.*,[10] which by character should not depend on initial amplitudes of the incoming 3-d disturbance. Strong amplification of fluctuating 3-d perturbations in the reference case should be attributed to nonlinear interaction merely to explain experimentally observed[12] growth rates, while transition is caused by the absolute instability.

Unlike in Wilson and Pauley,[5] Görtler vortices did not show up inside the separated region despite spanwise harmonic forcing. This raises doubt on the findings there, since the only evidence shown was a picture of instantaneous velocity contours at a far downstream position (close to the transition location, where the flow probably is already highly unsteady). The results here indicate that steady disturbances are rather streaks than vortices and can be expected only in the first part of the LSB, because fluctuations are far too high at reattachment to have curved streamlines. Furthermore, it appears that the formation of Görtler vortices can hardly be the route to shear-layer breakdown, unless in cases with extremely high initial amplitude (so-called bypass transition) as it was earlier argued to be necessary.

Our results do not contradict results of Pauley[4] that show an increased spanwise-averaged length of the separation bubble when adding spanwise sine-wave perturbations. Whereas they have compared two- and three-dimensional computations, in the present study all simulations, even those without forcing 3-d disturbances (e.g. case $A_{no\,3D}$), lead to immediate full three-dimensional breakdown of the shear-layer.

Present results support the second part of the conclusion in Ref. 11, that "simulations with forced Görtler modes may be misguided; and stationary imperfections in an experiment may not be harmful" (p. 348). In the light of our results, simulations with forced Görtler modes in a LSB are not misguided in the sence that they change the results but more in the sence that these vortices can be strongly forced and do appear, but are not relevant for the transition process.

Assuming that a similar transition mechanism in both cases is in operation, observations of this study suggest that a division into primary and secondary instability is meaningful despite the sudden break-up of the spanwise vortex into small-scale turbulence.

Acknowledgments

Financial support of this research by the Deutsche Forschungsgemeinschaft DFG under grant Wa 424/19–1 and Ri 680/10–1 is gratefully acknowledged. The authors would like to thank Matthias Lang for providing detailed experimental results.

References

[1]Watmuff, J., "Evolution of a Wave Packet into Vortex Loops in a Laminar Separation Bubble," *J. Fluid Mech.*, Vol. 397, 1999, pp. 119–169.

[2]Rist, U. and Maucher, U., "Investigations of time-growing instabilities in laminar separation bubbles," *Eur. J. Mech. B/Fluids*, Vol. 21, 2002, pp. 495–509.

[3]Inger, G., "Three-dimensional heat- and mass transfer effects across high-speed reattaching flows," *AIAA Journal*, Vol. 15, No. 3, 1977, pp. 383–389.

[4]Pauley, L., "Response of Two-Dimensional Separation to Three-Dimensional Disturbances," *J. Fluids Eng.*, Vol. 116, 1994, pp. 433–438.

[5]Wilson, P. and Pauley, L., "Two- and three-dimensional large-eddy simulations of a transitional separation bubble," *Phys. Fluids*, Vol. 10, No. 11, 1998, pp. 2932–2940.

[6]Reshotko, E., "Transient growth: A factor in bypass transition," *Phys. Fluids*, Vol. 13, No. 5, 2001, pp. 1067–1075.

[7]Boiko, A., "Development of a stationary streak in a local separation bubble," Tech. Rep. IB 224-2002 A04, German Aerospace Center (DLR), Institute for Fluid Mechanics, Göttingen, 2002.

[8]Yang, Z. and Voke, P., "Large-Eddy Simulation of Boundary-layer and Transition at a Change of Surface Curvature," *J. Fluid Mech.*, Vol. 439, 2001, pp. 305–333.

[9]Rist, U., "Nonlinear Effects of 2D and 3D Disturbances on Laminar Separation Bubbles," *Proceedings of IUTAM Symposium on Nonlinear Instability of Nonparallel flows*, edited by S. Lin, Springer, New York, 1994, pp. 324–333.

[10]Maucher, U., Rist, U., and Wagner, S., "Secondary Instabilities in a Laminar Separation Bubble," *Notes on Numerical Fluid Mechanics*, edited by H. Körner and R. Hilbig, Vol. 60, 10^{th}Stab Symposium 96, Braunschweig, Vieweg Verlag, Wiesbaden, 1997, pp. 229–236.

[11]Spalart, P. and Strelets, M., "Mechanisms of Transition and Heat Transfer in a Separation Bubble," *J. Fluid Mech.*, Vol. 403, 2000, pp. 329–349.

[12]Lang, M., Marxen, O., Rist, U., and Wagner, S., "Experimental and Numerical Investigations on Transition in a Laminar Separation Bubble," *New Results in Numerical and Experimental Fluid Mechanics III*, edited by Wagner, Rist, Heinemann, and Hilbig, 12^{th}Stab Symposium 2000, Stuttgart, NNFM 77 Springer-Verlag, Heidelberg, 2001, pp. 207–214.

[13]Marxen, O., Lang, M., Rist, U., and Wagner, S., "A Combined Experimental/Numerical Study of Unsteady Phenomena in a Laminar Separation Bubble," *submitted to Flow Turbul. Combust.*, 2002, Proceedings of IUTAM Symposium "Unsteady Separated Flows", Toulouse.

[14]Maucher, U., Rist, U., and Wagner, S., "Refined Interaction Method for Direct Numerical Simulation of Transition in Separation Bubbles," *AIAA Journal*, Vol. 38, No. 8, 2000, pp. 1385–1393.

[15]Kloker, M., "A robust high-resolution split-type compact FD scheme for spatial direct numerical simulation of boundary-layer transition," *Appl. Sci. Res.*, Vol. 59, 1998, pp. 353–377.

[16]Rist, U., Augustin, K., and Wagner, S., "Numerical Simulation of Laminar Separation-Bubble Control," *New Results in Numerical and Experimental Fluid Mechanics III*, edited by Wagner, Rist, Heinemann, and Hilbig, 12^{th}Stab Symposium 2000, Stuttgart, NNFM 77 Springer-Verlag, Heidelberg, 2001, pp. 181–188.

[17]Mendonça, M., Morris, P., and Pauley, L., "Interaction between Görtler vortices and two-dimensional Tollmien-Schlichting waves," *Phys. Fluids*, Vol. 12, 2000, pp. 1461–1471.

[18]Lee, K. and Liu, J., "On the growth of mushroomlike structures in nonlinear spatially developing Goertler vortex flows," *Phys. Fluids A*, Vol. 4, No. 1, 1992, pp. 95–103.

[19]Andersson, P., Brandt, L., Bottaro, A., and Henningson, D., "On the breakdown of boundary layer streaks," *J. Fluid Mech.*, Vol. 428, 2001, pp. 29–60.

[20]Gaster, M., "The structure and behaviour of laminar separation bubbles," *AGARD CP*, Vol. 4, 1966, pp. 813–854.

[21]Bakchinov, A., Grek, G., Klingmann, B., and Kozlov, V., "Transition experiments in a boundary layer with embedded streamwise vortices," *Phys. Fluids*, Vol. 7, No. 4, 1995, pp. 820–832.